

Electrochemical Characterization of Lithium Ferrite Electrodes through Cyclic Voltammetry and Raman Spectra

M. Manley & W. Cook

Department of Chemical Engineering, University of New Brunswick
Fredericton, NB, Canada, E3B 5A3

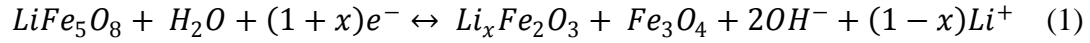
Summary

Lithium ferrite, a mixed spinel with the formula, $\text{Fe}[\text{Li}_{0.5}\text{Fe}_{1.5}]\text{O}_4$ or LiFe_5O_8 , has been synthesized and characterized in both its ordered (α) and disordered (β) phases. In an effort to scope the electrochemical activity lithium ferrite in lithium hydroxide solutions, the powders produced were compressed into pellets and tested with cyclic voltammetry and the surface of the electrodes were analyzed with laser Raman spectroscopy. Results of the initial electrochemical testing showed good correlation with Nernstian behavior and exhibited quasi-reversible behaviour. The redox mechanism involves the breakdown of lithium ferrite into hematite, a hybrid lithiated-hematite oxide and lithium ions under the alkaline conditions tested. By comparing the equilibrium potential of the redox process with proposed reaction schemes and examining the reaction products using the laser Raman microprobe, the proposed redox mechanism could be verified.

1. Introduction

Maintaining chemistry in a nuclear reactor coolant system, such as the primary heat transport (PHT) system in the Canadian designed CANDU reactor, is vital to the operation of the power plant. Of the many parameters that are monitored and controlled in the PHT system, the apparent pH (pH_a) in particular must be maintained within a narrow range in order to minimize the corrosion of the system materials. Ideally, the pH_a should be kept between 10.2 and 10.4 and is controlled by the addition of lithium hydroxide in order to achieve a corresponding lithium ion concentration between 0.34 and 0.55 ppm. It is proposed that a lithium ferrite electrode would be capable of measuring the lithium ion concentration and could potentially be used as a reference electrode for monitoring the electrochemical corrosion potential (ECP) of system materials, which would facilitate control of the delicate chemistry in the CANDU PHT system.

Lithium ferrite is a mixed spinel with the formula, $\text{Fe}[\text{Li}_{0.5}\text{Fe}_{1.5}]\text{O}_4$ or LiFe_5O_8 and is best used in its disordered, β -phase for electrochemical applications. In an effort to scope the electrochemical activity lithium ferrite in lithium hydroxide solutions, a previously prepared β - LiFe_5O_8 powder was compressed into pellets and tested using cyclic voltammetry. The surface composition of the electrodes was analyzed in-situ and ex-situ with Laser Raman spectroscopy. Aided by deconvolution of the Raman scans, the redox mechanism proposed involves the breakdown of lithium ferrite into hematite, a hybrid lithiated-hematite oxide and lithium ions under the alkaline conditions tested [equation (1)].



2. Background

In order to validate the proposed redox mechanism of the electrode, the redox products ($Li_xFe_2O_3$ and Fe_3O_4) needed to be physically identified. Various characterisation techniques have been employed to identify the phases present during lithiation of iron oxides. Nano-sized thin films of α - Fe_2O_3 (hematite) and α - Fe_2O_3 with Li^+ cations inserted in the matrix were investigated by Turkovic et al (1) for their importance in high capacity galvanic cells. Films of iron oxide were made by a chemical deposition method and investigated by impedance spectroscopy (IS), Raman, SEM, and XRD. Raman spectra were recorded using a Dilor Z24 Raman triple monochromator in a 45 degree scattering configuration using 2 W of cylindrically focused 514.5 nm argon ion laser. The study notes that the Raman frequencies were shifted upon addition of lithium to the hematite films, with the strongest peaks in the stabilized, lithiated films seen at 297 and 407 cm^{-1} . Shifts in the measured values to higher frequencies are attributed to the nanosized hematite particles and their ability to readily accept Li^+ ions into the crystal structure.

Magnetite, $Fe^{3+}(Fe^{2+}Fe^{3+})O_4$ is an inverse spinel with technologically significant properties, such as nonstoichiometry, order-disorder of cations between octahedral sites and oxidation, that can complicate its characterisation. In a study by Shebanova and Lazor(2), magnetite was investigated by vibrational spectroscopy in order to explain discrepancies reported for magnetite by several studies pertaining to its lattice dynamics. The authors used a pure sample of magnetite from a metamorphised iron formation. Impurities were measured and shown to be minimal (ppm) with mostly vanadium and titanium present. The x-ray diffraction measurements (XRD) were shown to be in good agreement with the reported literature values. Raman spectra were obtained by a 514.5 nm line of argon ion laser (Coherent, Innova) and were collected in a backscattering geometry with a spectral resolution of 6 cm^{-1} . The reported frequencies have uncertainties of $\pm 1.5 cm^{-1}$. The Raman results, under ambient conditions, showed the non-polarized spectrum of magnetite had four out of the five theoretically predicted bands at 668, 538, 306 and 193 cm^{-1} . From the table of reported Raman mode frequencies in the thirteen comparison studies, those in which magnetite was formed as a secondary product (four studies) as opposed to a pure sample, saw the expected 538 cm^{-1} peak shifted to 550 cm^{-1} . The table also showed that there was consistency among the strongest modes at 666, 538, and 306 cm^{-1} . The remaining modes were considered to be inconsistent between the studies. It is suggested by the authors that this may be due to the onset of oxidation in the sample, especially at the 410 and 1322 cm^{-1} modes as these are characteristic of hematite.

In a study by Pernet et al. (3), both chemical and electrochemical treatment of γ - Fe_2O_3 were performed to evaluate the maximum amount of lithium which could be added before the $Li_xFe_2O_3$ structure was compromised. Past a critical insertion number, iron and lithium are precipitated out of the transformed rock-salt structure. In specially produced nano-sized particles, insertion is significantly more reversible and, initially, the transformation into the rock-salt structure upon lithium insertion is suppressed; therefore, significantly more Li^+ atoms can be added before precipitation occurs (4). Chemical treatment of the γ - Fe_2O_3 particles was accomplished by mixing them with a 1.6 M solution of n-butyl lithium in hexane. The electrochemical treatment was done using slow

voltammetry in a solid electrolyte cell at 80°C. Lithium foil was used as the cathode and a 2:1 ratio of γ -Fe₂O₃: graphite was used as the anode in a LiClO₄ electrolyte. Lithium content in the particles was found to be $x=0.85$ - 0.87 in the chemically treated run and $x=1$ in the electrochemically treated run for Li_xFe₂O₃. The authors' explanation for a smaller concentration in the chemically treated sample is that the kinetics of lithium insertion and rock-salt transformation are very slow. The slow voltammetry (<40 mV/hour) promoted the kinetics reaching completion.

3. Experimental

To begin quantifying the reaction products, a potentiostatic experiment was performed for a period of 48 hours where the voltage was held at the equilibrium potential for the proposed reaction mechanism (Equation 1 – the equilibrium potential was determined to be -400 mV vs SCE from previous cyclic voltammetry experiments) while the working electrode (lithium-ferrite pellet) was being observed using the Raman microprobe attachment and cyclic voltammetry applied periodically. The lithium ferrite pellet used for this experiment was a β -LiFe₅O₈ (~52% beta phase) prepared using a nano-sized Fe₂O₃ powder as a starting material to ensure small particle size of the final product (~300 nm). This composition of lithium ferrite is denoted as n-LiFe₅O₈ for this study. Raman scans of the powder and pellet were done prior to electrochemical testing. Scans of the pellet's surface were also performed twice a day during the experiment and after the test was completed. The final spectra for the pellet and the original spectrum of the powder are shown for comparison in Figure 1.

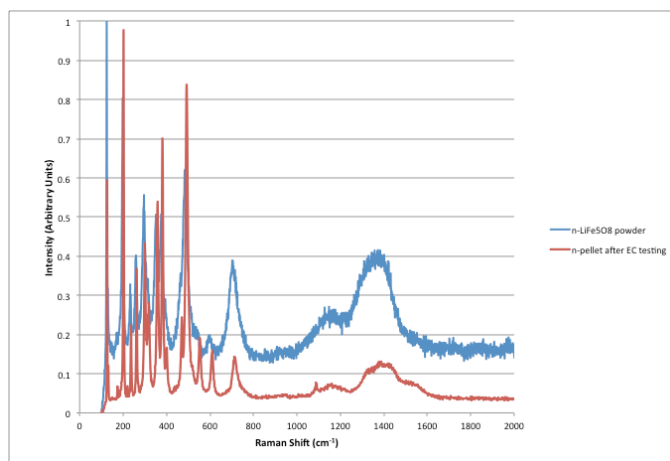


Figure 1: Comparison of normalized Raman spectra for original lithium ferrite powder and the lithium ferrite pellet after electrochemical testing.

From Figure 1, one can see that there are three peaks that immediately distinguish the two spectra. The scan of the pellet following the 48 hours of the potentiostatic application has additional peaks present at 400 cm⁻¹, 553 cm⁻¹ and 610 cm⁻¹ that are not observed in the original powder. Deconvolution of the powder and pellet Raman spectra in these specific ranges was done using Peakfit software to distinguish the presence of any hidden peaks. The deconvoluted Raman spectrum in the range of 200 - 400 cm⁻¹ and corresponding correlations between the actual data and deconvoluted data were high at 97.5% for the powder and 99.3% for the pellet and are shown in Figure 2.

The slightly lower correlation in the powder was due to a larger amount of noise in the original powder data.

A comparison of Figures 2(a) and (b) initially shows that the peaks at 309 and 400 cm^{-1} present on the scan of the pellet are not present on the scan of the lithium ferrite powder. The n-LiFe₅O₈ (β -phase LiFe₅O₈) has a characteristic peak around 400 cm^{-1} and upon closer examination of the comparative scans, this peak from the scan of the pellet can be attributed to a shift from the 393 cm^{-1} shoulder peak present in the powder; it is further observed that all the peaks on the pellet scan are shifted by approximately +6 cm^{-1} relative to the powder scan. In the study by Turkovic et al (1), 297 and 407 cm^{-1} have been identified as distinguishing peaks for lithiated hematite (LiFe₂O₃). In the experiment, thin films of Fe₂O₃ were doped with 0%, 1% and 10% Li⁺ ions. The resulting Raman scans showed shifted peaks indicative of lithiated hematite (LiFe₂O₃) at 297 and 407 cm^{-1} (1). Although the 400 cm^{-1} shift is indicative of both lithium ferrite and lithiated hematite, the peak at 309 cm^{-1} can only be representative of the lithiated hematite. The peaks at 372 and 388 cm^{-1} could be not be attributed to any relevant species. The peak at 372 cm^{-1} could possibly be a shifted peak of γ -Fe₂O₃, but it is more likely an artifact of the mathematical manipulation due to the two larger peaks being separated by more distance than in the powder. The peak at 388 cm^{-1} is likely an artifact due to the shift of the 400 cm^{-1} frequency.

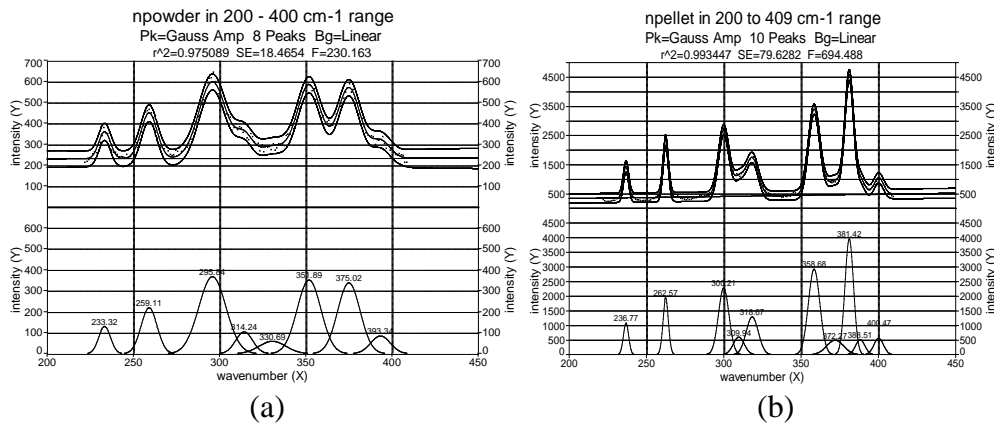
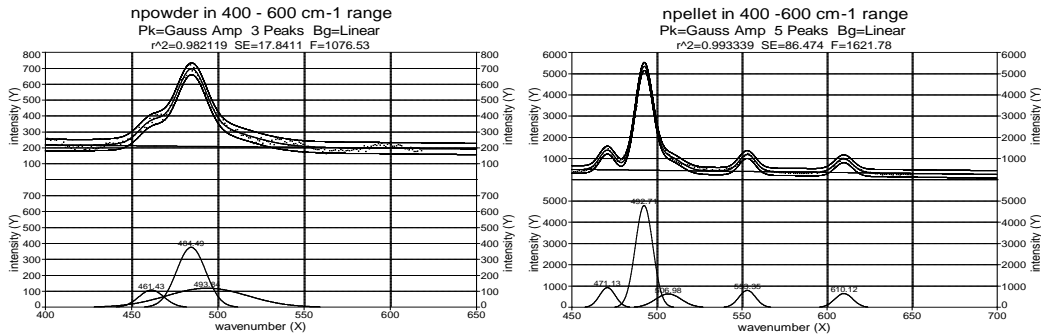


Figure 2(a) and (b): (a) Deconvolution of the Raman spectrum for the n-powder showing a correlation of 97.5% and a total of ten peaks 200 - 400 cm^{-1} range; (b) Deconvolution of the Raman spectrum for the n-pellet showing a correlation of 99.3% and a total of eight peaks in the 200 - 400 cm^{-1} range.

The comparison of Figures 3 (a) and (b) show the evolution of two new peaks at 553 and 610 cm^{-1} , which are distinguishing peaks for magnetite and hematite, respectively. As described above, in the review of magnetite Raman results by Shebanova and Lazor(2), the characteristic peak at 538 cm^{-1} for magnetite was measured at 550 cm^{-1} in experiments where magnetite was a secondary product. One of the identifying peaks for hematite is at 610 cm^{-1} .

Cyclic voltammetry revealed quasi-reversible behavior of the redox mechanism on the surface of the lithium ferrite electrode, as shown in the Figure 4(a). The cyclic voltammetry was run at various pH values to determine the effect of equilibrium potential on pH and therefore the Nernstian correlation. The results are shown in Figure 4(b).



Figures 3(a) and (b): (a) Deconvolution of the Raman spectrum for the n-powder showing a correlation of 98.2% and a total of three peaks in the 400-600 cm^{-1} range; (b) Deconvolution of the Raman spectrum for the n-pellet showing a correlations of 99.3% and a total of five peaks in the 400-600 cm^{-1} range.

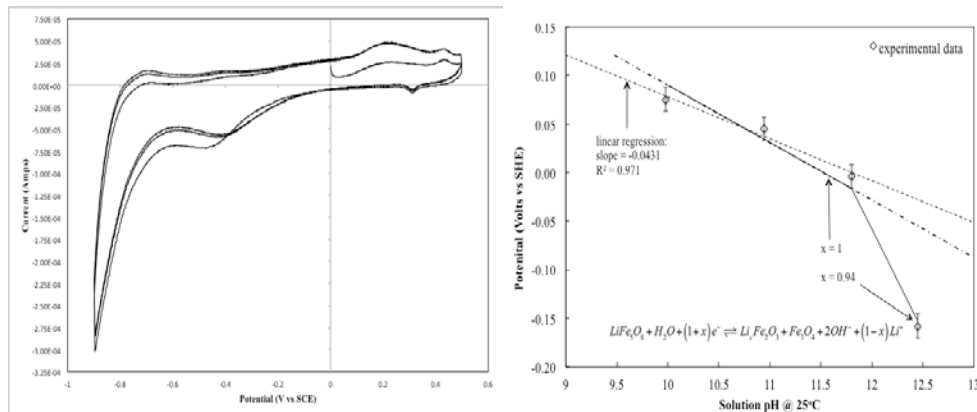


Figure 4(a) and (b): (a) Cyclic voltammogram run on lithium ferrite electrode; (b) Nernstian behavior of the lithium ferrite electrode and determination of non-stoichiometric reaction mechanism.

The presence of secondary peaks identified in the deconvoluted Raman spectra verify that both magnetite and hematite are present and that a form of lithiated-hematite (LiFe_2O_3) is likely present due to the shift identified at 309 cm^{-1} . This result physically confirmed the species present in the proposed reaction mechanism. The quasi-reversibility of the mechanism is illustrated in Figure 4(a) by the relative sizes and peak currents of the anodic and cathodic waves around -400 mV vs SCE . In a reversible reaction, both waves are identical with similar peak currents. Deviation in the plot of equilibrium potential versus pH in Figure 4(b) shows that the mechanism had non-stoichiometric behavior. The predicted potential versus pH behaviour when $x = 0.945$ at a lithium hydroxide concentration of 1.0 M is indicative that lithium ion insertion/desertion mechanism are more likely at the higher pH values.

Conclusions

The presence of the secondary peaks identified in the deconvoluted Raman spectra verify that both magnetite and hematite are present and that a form of lithiated-hematite (LiFe_2O_3) is likely present due to the shift identified at 309 cm^{-1} . It appears that, at room

temperature, the decomposition of lithium ferrite involves reduction of some of the ferric ions in the cubic lattice to produce a hybrid lithiated oxide, with lithiated-hematite being preferred. It is presumed that the hematite is most likely in the γ -Fe₂O₃ phase (maghemite), which would keep the cubic crystal structure of the lattice intact. To explain the deviation from Nernstian behaviour at high pH, a mechanism is proposed whereby the decomposition is non-stoichiometric and lithium ferrite is broken down into lithiated hematite with the partial release of lithium ions.

References:

1. A. Turkovic, M. Ivanda, M. Bitenc and Z. Crnjak, *J. Nanomater.*, **967307**, 2011 (2001).
2. O. N. Shebanova and P. Lazor, *J. Solid State Chem.*, **174**, 424 (2003).
3. M. Pernet, P. Strobel, B. Bonnet, P. Bordet and Y. Chabre, *Solid State Ionics.*, **66**, 259 (1993).
4. S. Kanzaki, T. Inada, T. Matsumuura, N. Sonoyama, A. Yamada and M. Jakano, *J. Power Sources.*, **146**, 323 (2005).